ACTA ACUSTICA UNITED WITH ACUSTICA
Vol. 92 (2006) 1047 – 1059

Physical Modeling of Buzzing Artificial Lips: The Effect of Acoustical Feedback

I. Lopez, A. Hirschberg
Eindhoven University of Technology, Den Dolech 2, 5612AZ Eindhoven, The Netherlands

A. Van Hirtum, N. Ruty, X. Pelorson
ICP UMR CNRS 5009 INPG/ Université Stendhal, 46 av. F. Viallet F-38031 Grenoble, France

Invited paper based on a presentation at Forum Acusticum 2005 in Budapest

Summary
The influence of the up- and downstream acoustics on the buzzing behavior of artificial lips has been studied. In the presence of a long downstream pipe, the oscillation frequency is well predicted by means of a model assuming a single mechanical degree of freedom for the lips. A minimum of the threshold pressure for buzzing is observed when the lips are just closed at rest. The magnitude of this threshold pressure is underestimated by the model. In order to fit experiments the quality factor of the lip resonance has to be reduced by a factor two compared to the measured quality factor. In the absence of downstream pipe the threshold pressure increases by a factor three and a jump in oscillation frequency from one mechanical lip-mode to another one is observed as the lung pressure is increased. An attempt to describe this behavior by means of a 2-mass-model fails.

PACS no. 43.75.Fg, 43.75.Yy

1. Introduction

Woodwind-instruments such as the clarinet or the oboe are driven by the oscillations of a valve, the reed, coupled to an acoustical resonator, the pipe. As the valve tends to close when the lung pressure is increased, Helmholtz [1] classified these valves as *inwards striking reeds*. Using a model with a single mechanical degree of freedom for the reed and a single acoustical resonance for the downstream pipe Helmholtz [1] predicted, by means of a linear stability analysis, that the instrument should sound at a frequency lower than both the reed and pipe resonance frequencies. This was verified by experiments. Helmholtz [1] postulated that lips in a brass instrument will have the opposite behavior, they are classified as *outward-striking reeds*, since they would open when the lung pressure is increased. This appears to be an oversimplification. Like the vocal folds, lips seem to have more than a single active mechanical degree of freedom [2, 3, 4, 5]. However, for many practical applications such as sound synthesis, one would like to use the most simple physical models of vocal fold oscillations to explain the behavior of lips in brass-instruments. The simple 2-mass model of Lous *et al.* [6] is an attractive candidate as it combines the essential features of fluid dynamics, such as a moving flow separation point, with a model for acoustical feedback from the upstream and downstream ducts.

Received 20 June 2005,
accepted 21 June 2005.

In the present paper we consider two different models: the single mechanical degree of freedom model proposed by Cullen *et al.* [5] and the 2-mass model of Lous *et al.* [6]. The parameters needed for these models have been determined from static and dynamic measurements on artificial lips. Then a linear stability analysis has been carried out with both models to predict the onset of self-sustained oscillations of the lips. These results have been compared to measured data from the artificial lips. The effect of acoustical feedback has been studied by performing measurements and simulations for different lengths of a downstream pipe connected to the artificial lips.

We used in our experiments an artificial lip based on latex tubes filled with water as used by Gilbert *et al.* [7] and Cullen *et al.* [5]. We used however a modification inspired by the work of Vergez [8]: the lip tension is imposed by controlling the internal water pressure rather than by imposing a mechanical constraint. This set-up has not necessarily more realistic mechanical boundary conditions than the model of Gilbert *et al.* [7], but these boundary conditions are easier to control. Another major difference between our set-up and the set-up of Gilbert *et al.* [7] is that we use an artificial upper airways (vocal track/trachea) and a large volume representing the lungs. This provides a more realistic upstream acoustical behavior.

The paper is organized as follows: the experimental set-up and measurement procedure is explained in section 2. In section 3 the 1-mass model of Cullen *et al.* [5] is shortly presented, while the 2-mass model of Lous *et al.* [6] with upstream and downstream pipes is described in section 4.

Both the experimental and numerical results are presented in section 5 and in section 6 the dynamic behavior of the 2-mass model of Lous *et al.* [6] is discussed. Finally, the main conclusions are summarized in section 7.

2. Experimental procedure

The artificial lips sketched in Figure 1 are described by Vilain *et al.* [9]. The lips consist of latex tubes of 1 cm diameter and 0.3 mm wall thickness. Each tube is mounted on a metal cylinder, the lip-holder, of 1 cm internal diameter. Half of this cylinder has been removed over a length of $b = 3$ cm corresponding to the length of the lips in the direction transversal to the flow. A central duct of 2 mm diameter along the axis of the cylinder allows to fill the lips with water. The lip-holders are mounted in cylindrical holes drilled in a metal block. A global sketch of the set up is provided in Figure 2. A pipe of length $L_u = 30$ cm and a diameter $d_u \cong 3$ cm representing the upper airways, connects the lip-model to a reservoir of volume $V_l = 0.68$ m^3 representing the lungs. The diameter d_u is not uniform because a laser is placed in this pipe section. The upstream reservoir is filled with acoustical foam in order to avoid resonances. The static pressure p_l in the reservoir is adjusted by a regulating valve feeded by a high pressure reservoir (8 bar). The lung pressure was measured within an accuracy of 20 Pa by means of a water manometer.

Experiments have been performed without downstream pipe ($L_d = 0$), a short pipe ($L_d = 16$ cm) and a long pipe ($L_d = 49$ cm). The downstream pipe had a diameter of $d_d = 3$ cm. The acoustical response of the upstream pipe has been determined experimentally. When the lips are closed, this pipe segment has a quarter-wavelength resonance at a frequency $f_u = 240$ Hz with a quality factor $Q_u = 5$.

The internal lip-pressure p_{in} is imposed before each experiment by adjusting the level of a water reservoir connected to the lips (Figure 1). This adjustment is carried out at zero lung pressure. The valve connecting the lips to the water reservoir is then closed. The lips remain connected to each other through the water feeding duct. This keeps the lip tension equal while the water volume remains fixed. We call this the constant volume operation mode [9]. The pressures in the airways just upstream of the lips p_u and just downstream of the lips p_d were measured by means of Kulite pressure gages (type XCS093). The lip opening h was monitored by means of an optical system similar to the one used by Cullen *et al.* [5]. A laser diode (type ACM1 (635-3) 1 mW) has been build within the upstream pipe segment (Figure 2). The intensity of the light passing through the lip opening is recorded. A lens placed in front of the photodiode captures the diffracted light for lip openings larger than 10^{-5} m. The optical system is calibrated by traversing a razor blade mounted on a micrometer, through the beam. The derivative of the diode signal I with respect to the position of the razor blade provides the sensitivity ($\mathrm{d}I/\mathrm{d}x$) of the setup. In first approximation $\mathrm{d}I/\mathrm{d}x$ is constant within the range of lip opening

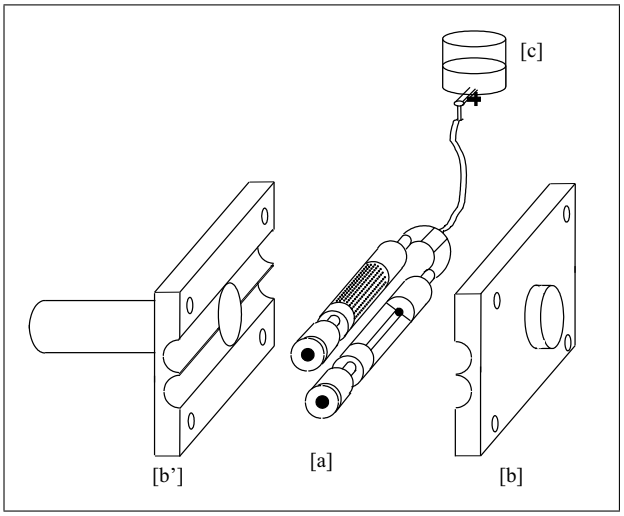

Figure 1. Schematic representation of the lips. a: lip replica, b,b': metallic block (lip holder), c: water reservoir.

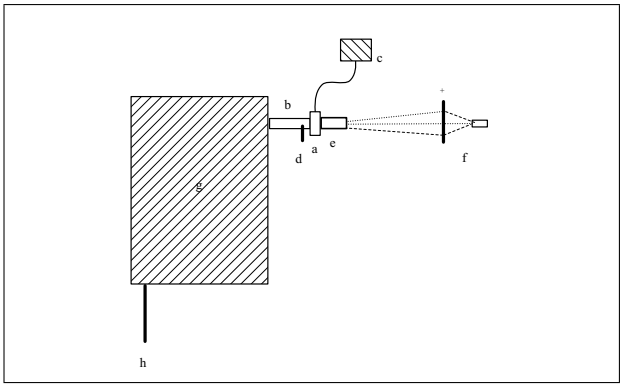

Figure 2. Schematic representation of the test setup. a: lip replica, b: upstream pipe/laser, c: water reservoir (internal lip pressure), d: upstream pressure gauge, e: downstream pipe, f: lens and photodiode, g: lungs (pressure reservoir), h: high pressure air supply line.

considered. For an internal lip pressure $p_{in} = 9.1$ kPa we find from static measurements a lip opening $h = Cp_l$ with $C = 3.5 \times 10^{-8}$ mPa^{-1}. An overview of the static measurement of the lip opening as a function of the lip pressure p_l is given in Figure 3.

During dynamical experiments, the lip oscillation frequency was determined from the laser signal. The transfer function between the lip opening h and a broad band noise signal driving a set of loudspeakers placed just downstream of the lips as shown in Figure 4 ($L_d = 0$) is used to determine the mechanical response of the lips. During those measurements, the lips were attached by means of the upstream pipe segment (L_u) to the reservoir (lungs). The response obtained will therefore combine the mechanical response of the lips with the acoustical response of the vocal tract and lungs. For the data acquisition and analysis we used a HP 3635 analyzer. The measurement of the mechanical response of the lips is limited to internal lip pressures below $p_{in} = 9.1$ kPa. At this pressure the lips are just closed when $p_l = 0$. The lung pressure thresh-

old $p_l = p_{th}$ at the onset of self sustained oscillation was determined by detecting the sound production of the set-up (Figure 2). The occurrence of self-sustained oscillation could also be confirmed by the appearance of a line spectrum in the frequency response of the lips. However, the acoustic detection was used because it was found to be more convenient in practice.

3. One-mass model

The model proposed by Cullen *et al.* [5] has been used to predict the self-sustained oscillation of the lips. This is originally a two degree of freedom (DOF) model: one mechanical DOF for the lips and a second for the acoustics. The mechanical behavior of the lips is modeled as a one DOF spring-mass-damper system. We assume that the two lips are identical and that their movement is symmetrical (opposite phase). The acoustics of the downstream pipe is described by assuming a single acoustical resonance following the approximation of Cullen *et al.* [5]. We use the same approach to take the acoustical response of the upstream pipe into account when there is no downstream pipe ($L_d = 0$). Following Fletcher and Rossing [4] the dynamics of an outwards striking reed is described by the equation

$$\frac{\mathrm{d}^2 h'}{\mathrm{d}t^2} + \frac{\omega_L}{Q_L}\frac{\mathrm{d}h'}{\mathrm{d}t} + \omega_L^2 h' = -A_d p'_d + A_u p'_u, \qquad (1)$$

where h' is the fluctuation in the opening h of the lips, ω_L is the natural frequency of the lips, Q_L is the quality factor of the lip resonance, p'_d and p'_u are the fluctuating parts of respectively p_d and p_u (where u and d stand for the upstream and downstream pipe respectively) and A_d and A_u are the corresponding ratios of the effective surface areas, on which the pressure acts and of the effective mass of the lips. We neglect steady flow pressure losses in the ducts.

The downstream pressure oscillates around the atmospheric pressure $p'_d = p_d$. Upstream of the lips we have $p'_u = p_u - p_l$. The factors A_d and A_u are positive for an outward striking valve. In principle $A_u \neq A_d$. As noted by Fletcher and Rossing [4] a model of the lips in which $A_d < 0$ cannot be excluded.

The acoustical system is described by the following equation [5]:

$$\frac{\mathrm{d}^2\psi}{\mathrm{d}t^2} + \frac{\omega_i}{Q_i}\frac{\mathrm{d}\psi}{\mathrm{d}t} + \omega_i^2\psi = \frac{Z_i\omega_i}{Q_i}\phi'_i, \quad (i = u, d), \quad (2)$$

where $(d\psi/dt) = p'_i$, $\omega_i = 2\pi f_i$ is the acoustical resonance frequency, Q_i is the quality factor, Z_i is the peak value of the acoustical impedance at ω_i and ϕ'_i is the unsteady component of the volume flow through the lips. Neglecting the compressibility of the flow and the volume displacement by the movement of the lips, we have by conservation of volume flow $\phi'_u = -\phi'_d$. Using a quasi-steady incompressible flow approximation we obtain

$$\phi'_d = -\phi'_u = bh'U_B - \frac{bh_0}{\rho U_B}(p'_d - p'_u), \qquad (3)$$

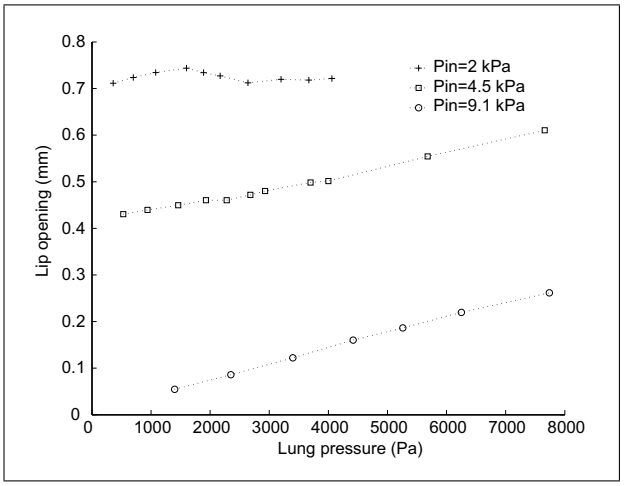

Figure 3. Static measurements of lip opening vs lung pressure for different values of the internal lip pressure p_{in} =2, 4.5 and 9.1 kPa.

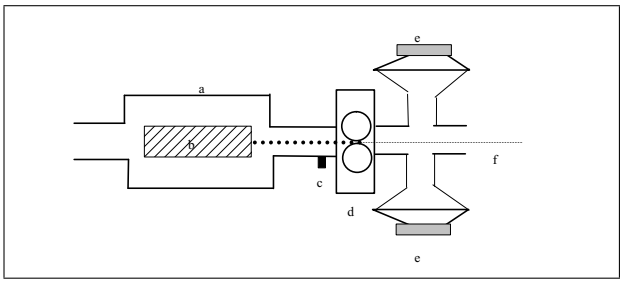

Figure 4. Schematic representation of the test setup for the transfer function measurements. a: upstream pipe, b: laser, c: upstream pressure gauge, d: lip replica, e: loudspeakers, f: transmitted laser beam.

where $h_0 = h - h'$, U_B is the mean value of the flow velocity. We implicitly assume flow separation followed by a dissipation of the kinetic energy without pressure recovery in a free jet of thickness h and width b. The flow velocity U_B is calculated by means of the equation of Bernoulli,

$$U_B = \sqrt{\frac{2p_l}{\rho}}, \qquad (4)$$

where $\rho = 1.2\ \mathrm{kg/m^3}$ is the density of the air. The acoustical impedance Z_u of the upstream pipe has been determined from measurements of the resonance frequency and the quality factors of a long pipe (4 m) attached to the reservoir. The impedance Z_d of the downstream pipe was calculated assuming radiation of an unflanged pipe in free space and taking visco-thermal losses in the pipe into account [10]. Linear stability theory is used to determine the lung pressure p_{th} at the threshold for oscillation and the oscillation frequency f from equations (1), (2) and (3). We assume a solution with a time dependence $\exp(\alpha t)$. When we seek for the threshold behavior we assume $\alpha = i\omega$ and we solve for p_{th} and ω. For a given $p_l > p_{th}$ we solve the system of equations for α and assume $\omega = \Im[\alpha]$. In the present paper, and for the single mass model, we consider only calculations with either $p'_u = 0$ or $p'_d = 0$.

4. Two-mass model

4.1. Acoustics and flow model

In the present work the 2-mass model of the lips has been coupled to two pipes, one upstream and one downstream of the lips. An schematic view is given in Figure 5.

These two pipes have been modeled as 1 DOF acoustic systems following the same strategy explained in section 3. The acoustic response of each of the pipes can be modeled using equation (2). In order to determine the parameters Q_i, Z_i and ω_i the impedance at the lip side of each of the pipes has to be found.

The upstream pipe is connected to a reservoir which models the lungs and the reflection coefficient R is known from previous work (Figure 6). Therefore, the impedance at the lip side of the pipe is given by [10, 4]

$$Z_1(x=0^-) = \frac{p'_u}{\phi'_v} = -\frac{\rho_0 c_0}{S_p}\frac{R\mathrm{e}^{-2\mathrm{i}kL_1}+1}{R\mathrm{e}^{-2\mathrm{i}kL_1}-1}. \qquad (5)$$

The downstream pipe has an open end with a (known) impedance Z_{out}. For Z_{out} we use the low frequency approximation $Z_{out} = (\rho_0 c_0/S_p)\left((ka)^2/4 + \mathrm{i}k\delta\right)$ for an unflanged open pipe termination with pipe cross-section radius a and end correction $\delta = 0.7a$ [11]. The impedance at the lip side of the downstream pipe is

$$Z_2(x=0^+) = \frac{\rho_0 c_0}{S_p}\frac{Z_{out}\left(1+\mathrm{e}^{-2\mathrm{i}kL_2}\right)+\frac{\rho_0 c_0}{S_p}\left(1-\mathrm{e}^{-2\mathrm{i}kL_2}\right)}{Z_{out}\left(1-\mathrm{e}^{-2\mathrm{i}kL_2}\right)+\frac{\rho_0 c_0}{S_p}\left(1+\mathrm{e}^{-2\mathrm{i}kL_2}\right)}. \qquad (6)$$

A curve fit of the resonance peak of the impedances given by equations (5) and (6) has been performed to obtain the parameters Q_u, Z_u and ω_u and Q_d, Z_d and ω_d.

The flow through the lips is modeled in the same way explained in section 3 leading to equation (3). The lip opening at rest, h_0, is in the 2-mass model given by the equilibrium distance $\overline{h_2}$ between the two downstream masses.

4.2. Mechanical model

The 2-mass model considered here is a symmetric model as shown in Figure 7. Two identical masses m are attached to identical spring k/damper c combinations. The masses can only move vertically and the interaction force between the two masses is proportional to the difference in vertical displacement (spring constant $k_c = k_\theta/(x_2 - x_1)^2$). Furthermore, the two lips are assumed to be identical and to move symmetrically. The dynamic equations of this system can be written as follows:

$$\begin{cases} m\ddot{y}_1 + c\dot{y}_1 + (k+k_c)y_1 - k_c y_2 \\ \qquad = F_1(y_1, y_2, P_u, P_d), \\ m\ddot{y}_2 + c\dot{y}_2 + (k+k_c)y_2 - k_c y_1 \\ \qquad = F_2(y_1, y_2, P_u, P_d), \end{cases} \qquad (7)$$

where m, c and k are the mass, damping coefficient and stiffness coefficient respectively and k_c is the coupling stiffness between the two masses. The force terms F_1 and F_2 have been calculated using the expressions given in [6]. This model assumes that the masses support straight massless walls.

For small variations around the equilibrium position the displacements of the two masses are:

$$\begin{aligned} y_1 &= \overline{y_1} + y'_1, \\ y_2 &= \overline{y_2} + y'_2, \end{aligned} \qquad (8)$$

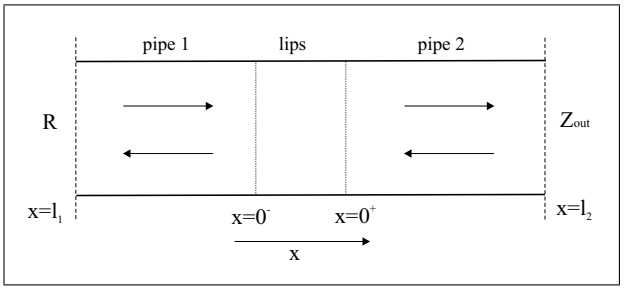

Figure 5. Acoustical model.

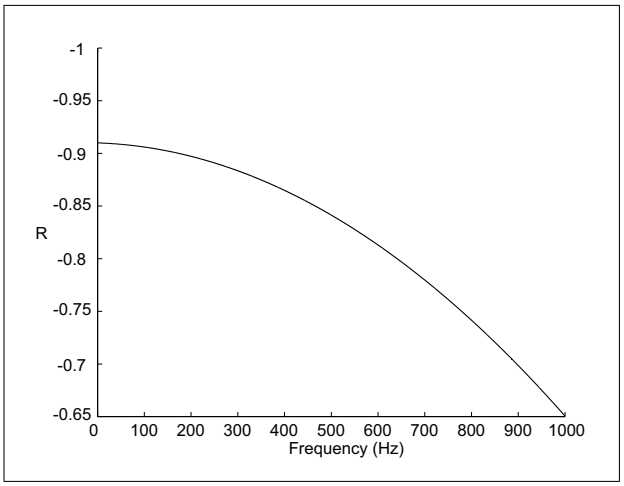

Figure 6. Average measured reflection coefficient.

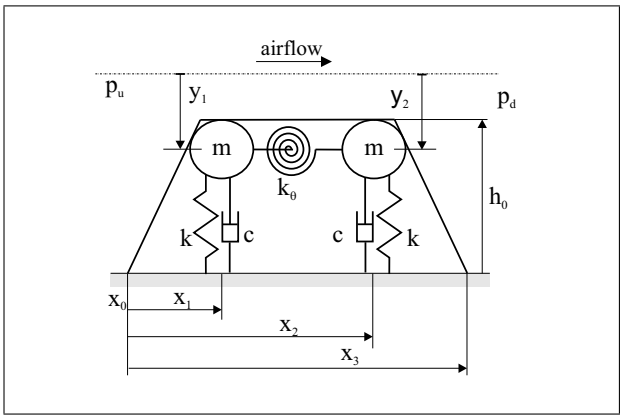

Figure 7. 2-mass model of Lous *et al.* [6].

and equations (7) become:

$$\begin{cases} m\ddot{y}_1' + c\dot{y}_1' + (k+k_c)y_1' - k_c y_2' = \\ \quad \left.\frac{\partial F_1}{\partial y_1}\right|_{(\overline{y_1},\overline{y_2},\overline{P_u},0)} y_1' + \left.\frac{\partial F_1}{\partial y_2}\right|_{(\overline{y_1},\overline{y_2},\overline{P_u},0)} y_2' \\ \quad + \left.\frac{\partial F_1}{\partial P_u}\right|_{(\overline{y_1},\overline{y_2},\overline{P_u},0)} p_u' + \left.\frac{\partial F_1}{\partial P_d}\right|_{(\overline{y_1},\overline{y_2},\overline{P_u},0)} p_d', \\ m\ddot{y}_2' + c\dot{y}_2' + (k+k_c)y_2' - k_c y_1' = \\ \quad \left.\frac{\partial F_2}{\partial y_1}\right|_{(\overline{y_1},\overline{y_2},\overline{P_u},0)} y_1' + \left.\frac{\partial F_2}{\partial y_2}\right|_{(\overline{y_1},\overline{y_2},\overline{P_u},0)} y_2' \\ \quad + \left.\frac{\partial F_2}{\partial P_u}\right|_{(\overline{y_1},\overline{y_2},\overline{P_u},0)} p_u' + \left.\frac{\partial F_2}{\partial P_d}\right|_{(\overline{y_1},\overline{y_2},\overline{P_u},0)} p_d'. \end{cases} \quad (9)$$

Expressions for the derivatives of the forces F_1 and F_2 are given in the Appendix. The following equation can be used to determine the equilibrium position:

$$\begin{cases} (k+k_c)\overline{y_1} - k_c\overline{y_2} = F_1\left(\overline{y_1}, \overline{y_2}, \overline{P_u}, 0\right), \\ -k_c\overline{y_1} + (k+k_c)\overline{y_2} = F_2\left(\overline{y_1}, \overline{y_2}, \overline{P_u}, 0\right), \end{cases} \quad (10)$$

where the overbars indicate the equilibrium values. We assume that in absence of a pressure difference ($\overline{P_u} = \overline{P_d}$) the equilibrium positions are $\overline{y_{10}} = \overline{y_{20}} = 0$ ($\overline{h_{10}} = \overline{h_{20}} = 0$). Furthermore, the equilibrium distance between the two downstream masses $\overline{h_2}$ is equal to twice the equilibrium vertical displacement $\overline{y_2}$ ($\overline{h_2} = 2\overline{y_2}$).

4.3. Total coupled model

The total coupled model has 4 degrees of freedom (DOF): 2 mechanical DOF's (y_1, y_2) and 2 acoustical DOF's (ψ_d, ψ_u).

$$\begin{cases} m\ddot{y}_1' + c\dot{y}_1' - \frac{\partial F_1}{\partial P_u}\dot{\psi}_u' - \frac{\partial F_1}{\partial P_d}\dot{\psi}_d' \\ + \left(k + k_c - \frac{\partial F_1}{dy_1}\right) y_1' - \left(k_c + \frac{\partial F_1}{dy_2}\right) y_2' = 0, \\ m\ddot{y}_2' + c\dot{y}_2' - \frac{\partial F_2}{\partial P_u}\dot{\psi}_u' - \frac{\partial F_2}{\partial P_d}\dot{\psi}_d' \\ - \left(k_c + \frac{\partial F_2}{dy_1}\right) y_1' + \left(k + k_c - \frac{\partial F_2}{dy_2}\right) y_2' = 0, \\ \ddot{\psi}_u' + \left[\frac{\omega_u}{Q_u} + \frac{Z_u\omega_u}{Q_u}\frac{L\overline{h_2}}{\rho\overline{U_3}}\right]\dot{\psi}_u' \\ - \frac{Z_u\omega_u}{Q_u}\frac{L\overline{h_2}}{\rho\overline{U_3}}\dot{\psi}_d' + 2\frac{Z_u\omega_u}{Q_u}L\overline{U_3}y_2' + \omega_u^2\psi_u' = 0, \\ \ddot{\psi}_d' - \frac{Z_d\omega_d}{Q_d}\frac{L\overline{h_2}}{\rho\overline{U_3}}\dot{\psi}_u' + \left[\frac{\omega_d}{Q_d} + \frac{Z_d\omega_d}{Q_d}\frac{L\overline{h_2}}{\rho\overline{U_3}}\right]\dot{\psi}_d' \\ \qquad -2\frac{Z_d\omega_d}{Q_d}L\overline{U_3}y_2' + \omega_d^2\psi_d' = 0, \end{cases} \quad (11)$$

where $h_2 = 2y_2$ has been used. While the original model of Lous *et al.* [6] describes a moving flow separation point for large oscillation amplitudes, in linearized theory, as used here, the separation point remains fixed at the downstream end (mass 2).

Equation (11) can be written in state-space form:

$$\dot{x} = Ax, \quad (12)$$

where $x = [y_1, y_2, \psi_u, \psi_d, \dot{y}_1, \dot{y}_2, \dot{\psi}_u, \dot{\psi}_d]^T$ and A is given by

$$A = \left[\begin{array}{cccc|cccc} 0 & 0 & 0 & 0 & 1 & 0 & 0 & 0 \\ 0 & 0 & 0 & 0 & 0 & 1 & 0 & 0 \\ 0 & 0 & 0 & 0 & 0 & 0 & 1 & 0 \\ 0 & 0 & 0 & 0 & 0 & 0 & 0 & 1 \\ \hline -\frac{k+k_c-\frac{\partial F_1}{dy_1}}{m} & \frac{k_c+\frac{\partial F_1}{dy_2}}{m} & 0 & 0 & \frac{-c}{m} & 0 & \frac{1}{m}\frac{\partial F_1}{\partial P_u} & \frac{1}{m}\frac{\partial F_1}{\partial P_d} \\ \frac{k_c+\frac{\partial F_2}{dy_1}}{m} & -\frac{k+k_c-\frac{\partial F_2}{dy_2}}{m} & 0 & 0 & 0 & \frac{-c}{m} & \frac{1}{m}\frac{\partial F_2}{\partial P_u} & \frac{1}{m}\frac{\partial F_2}{\partial P_d} \\ 0 & -2\frac{Z_u\omega_u}{Q_u}L\overline{U_3} & -\omega_u^2 & 0 & 0 & -\left[\frac{\omega_u}{Q_u} + \frac{Z_u\omega_u}{Q_u}\frac{L\overline{h_2}}{\rho\overline{U_3}}\right] & \frac{Z_u\omega_u}{Q_u}\frac{L\overline{h_2}}{\rho\overline{U_3}} & \\ 0 & 2\frac{Z_d\omega_d}{Q_d}L\overline{U_3} & 0 & -\omega_d^2 & 0 & 0 & \frac{Z_d\omega_d}{Q_d}\frac{L\overline{h_2}}{\rho\overline{U_3}} & -\left[\frac{\omega_d}{Q_d} + \frac{Z_d\omega_d}{Q_d}\frac{L\overline{h_2}}{\rho\overline{U_3}}\right] \end{array}\right]$$

The same procedure explained in section 3 can be used to carry out a linear stability analysis by calculating the eigenvalues of A and looking at the sign of their real part.

5. Results

5.1. Experimental results

In this section the experimental results will be compared to the predictions obtained by means of the single mass model of Cullen *et al.* [5] presented in the previous section. In Figure 8 the measured transfer function between h' and p_d' is shown for four different lung pressures p_l = 0 Pa, 1.13 kPa, 2.50 kPa and 3.44 kPa. Those data correspond to the situation without a downstream pipe and an internal lip pressure p_{in} = 9.1 kPa. At rest ($p_l = 0$) the lips are just closed.

Three resonance peaks can clearly be distinguished both in the magnitude and phase plots. The frequencies of these peaks are for $p_l = 0$ approximately f_1 = 80 Hz, f_2 = 160 Hz and f_3 = 220 Hz. These frequencies increase with increasing lung pressure p_l. Cullen *et al.* [5] also found three resonance peaks, but with higher frequencies. The quality factors Q_i (i=1,2,3) of the resonance peaks have been estimated from the 3-dB bandwidth. Values between 3 and 10 have been obtained depending on the internal lip pressure p_{in}. These values are lower than those reported by Cullen *et al.* [5]. Once f_i and Q_i are known we follow the procedure of Cullen *et al.* [5] to determine A_d and the character of the peak (inward- or outward-striking). Under the assumption that each resonance can be independently modeled, they determine the character of the peak from the phase of the transfer function between mouth pressure (upstream) oscillations and lip opening [12, 3]. In [5] a

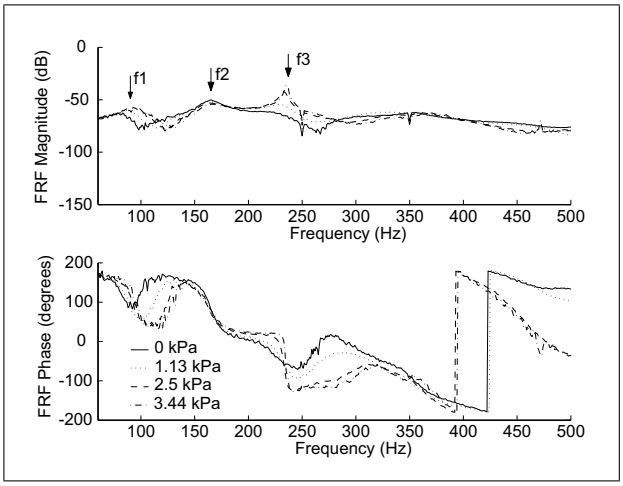

Figure 8. Measured frequency response functions between lip opening h and the downstream pressure p_d for several lung pressures p_l, no downstream pipe and an internal lip pressure p_{in} = 9.1 kPa: amplitude (dB re 10^{-7} Pa, upper) and phase (lower).

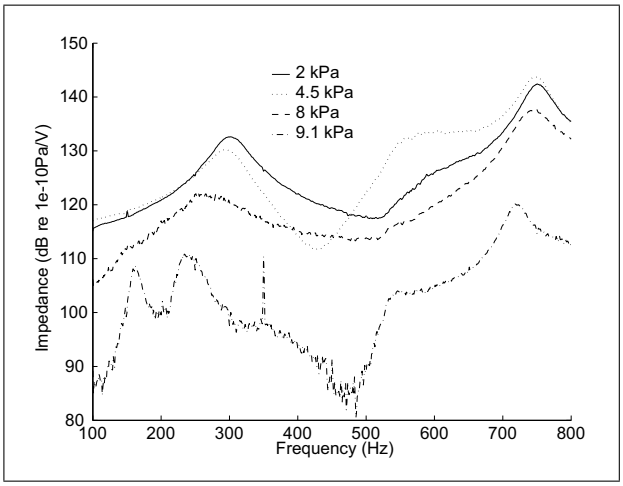

Figure 9. Measured impedance for the upstream pipe. p_{in} = 2, 4.5, 8, 9.1 kPa.

negative phase indicates outward-striking behavior and a positive phase an inward-striking character. The transfer functions shown in Figure 8 correspond to a pressure oscillation downstream, which means that the signs must be switched: a positive phase means outward-striking behavior and a negative phase inward-striking behavior. The values of the area factor A_d were ranging from $A_d = 0.03$ to 0.08 m^2kg^{-1} depending on p_{in}. This is lower than the values found by Cullen *et al.* [5]. Regarding the character of the resonances, we have found that the first two peaks display an outward-striking behavior, while the third has an inward-striking behavior. This contrasts with the observation of Cullen *et al.* [5] that the first peak had an outward-striking character and the other peaks had inward-striking characters. This might reflect the difference in mechanical boundary conditions of the lips in the two set-ups.

The upstream pipe segment does not have a uniform cross-section along its length, because the laser has been built within this pipe, as explained in section 2. In order

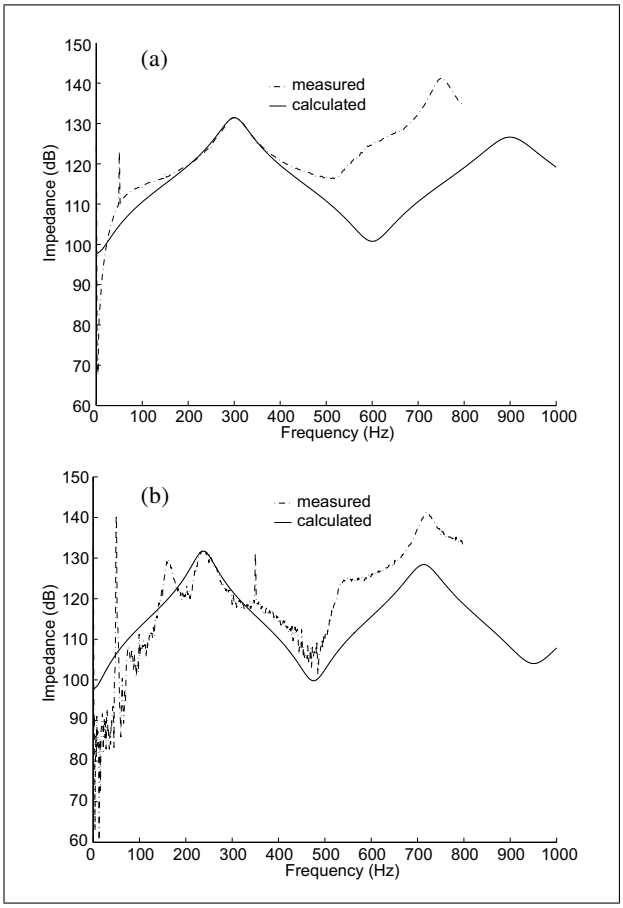

Figure 10. Comparison of measured and predicted (dB / 1 Pa s/m) impedance for the upstream pipe. (a) p_{in} = 2 kPa (measured data dB re 1.14e-10), (b) p_{in} = 9.1 kPa (measured data dB re 8.9e-12).

to have an estimate of the acoustical properties of this pipe, measurements of the acoustical impedance upstream of the lip model have been performed. This impedance has been estimated from the ratio of the pressure measured upstream of the lip model and the electrical signal driving to the loudspeaker downstream (which is related to the velocity), without a downstream pipe. In Figure 9 the measured impedance for four different values of the internal lip pressure p_{in} is shown. The first resonance frequency decreases from 300 to 240 Hz as the lips go from open to closed. For an internal lip pressure p_{in} = 9.1 kPa an additional peak at about 160 Hz can be seen. This corresponds to the second mechanical resonance f_2 of the lips (see Figure 8). The fact that the upstream pipe is excited indicates a movement in the direction of the pipe axis, which stresses the difference between this second lip mode and the other two modes, which do not appear in the upstream pressure response to excitation downstream.

In order to generate the necessary input data for the model, the theoretical input impedance for a pipe with a known reflection coefficient at one side and an open-end at the other side has been calculated. Experimental data for the reflection coefficient has been used (Figure 6). The length of the pipe has been chosen to fit the mea-

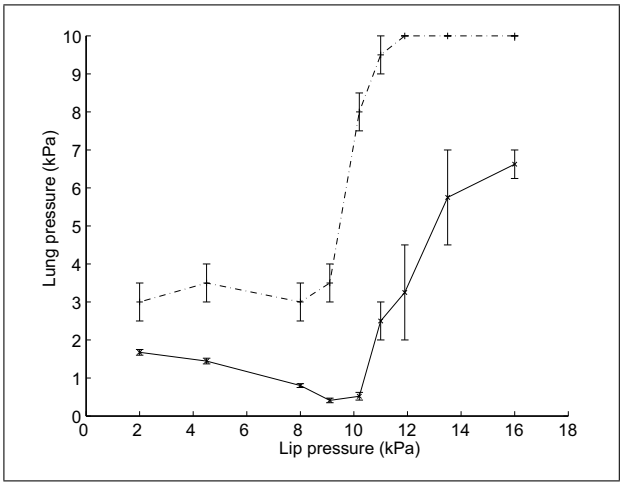

Figure 11. Lung pressure threshold p_{th} for oscillation as a function of the internal lip pressure p_{in}, measured without pipe L_d = 0 cm (-.-) and with a long pipe L_d = 49 cm (—).

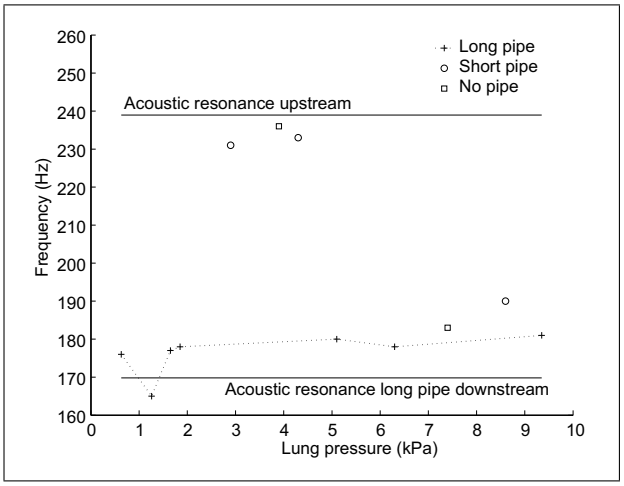

Figure 12. Influence of the downstream pipe length L_d on the measured oscillation frequency f as a function of the lung pressure p_l for an internal lip pressure p_{in} = 9.1 kPa (no pipe L_d = 0, short pipe L_d = 16 cm, long pipe L_d = 49 cm).

sured resonance frequencies. The measured and calculated impedance for two different values of p_{in} are shown in Figure 10. The experimental curve has been shifted to enable comparison. The prediction of the quality factor based on the measured reflection coefficient is satisfactory.

The lung pressure threshold p_{th} for the onset of self sustained oscillations and the frequency f of these oscillations have been measured for several different lip pressures and three different downstream pipe lengths (L_d = 0 cm, 16 cm and 49 cm). In Figure 11, the threshold pressure p_{th} is shown as a function of the internal lip pressure p_{in} for L_d = 0 cm and 49 cm. The results for a short pipe L_d = 16 cm cannot be distinguished from those without pipe L_d = 0 cm.

Figure 11 shows that, for a long pipe L_d = 49 cm, the lung pressure threshold p_{th} decreases as the internal lip pressure p_{in} increases until a minimum is reached at $(p_{in})_{critical}$ = 9.1 kPa. At this critical point the lips are just closed at rest, when p_l = 0. If p_{in} is further increased the threshold pressure p_{th} increases rapidly. In practice, for a musician, this minimum threshold pressure would be related to an optimal configuration for the ease of playing. In the absence of a downstream pipe L_d = 0 the threshold pressure is about a factor three larger than with a pipe. The uncertainty in p_{th} is larger without pipe L_d = 0 than with pipe L_d = 49 cm, which reflects the fact that the oscillation threshold is less acute.

The oscillations are less stable without downstream pipe. This again corresponds to the common experience of brass-instrument players: the lip oscillation is indeed considerably easier with the instrument attached to the embouchure than without.

Figure 12 shows the influence of the downstream pipe length L_d on the frequency f of self-sustained oscillation as a function of the lung pressure p_l for an internal lip pressure p_{in} = 9.1 kPa. The quarter wavelength resonance frequency of the upstream pipe f_u = 240 Hz and the quarter wavelength resonance frequency of the long pipe f_d = 170 Hz are shown as references. We see that for the long pipe L_d = 49 cm, the oscillation frequency is fairly constant and close to the pipe resonance. For the short pipe L_d = 16 cm and no pipe L_d = 0, two different oscillation modes are observed depending on the lung pressure p_l. For p_l < 5 kPa frequencies around f = 235 Hz are observed, close to the third lip resonance f_3 = 220 Hz (see Figure 8). Above p_l = 7 kPa the oscillation frequency drops to a frequency of around f = 185 Hz, close to the second lip resonance f_2 = 160 Hz.

5.2. One-mass model

The data obtained from the transfer function measurements has been used as input for the single-mass model described in section 3. A linear stability analysis is used to predict the threshold pressure p_{th} for self-sustained oscillation frequency and the corresponding oscillation frequency f. The resonance frequency f_2 of the second lip resonance in Figure 8 has been chosen for the mechanical model. The upstream pressure fluctuations are neglected: p'_u = 0.

In Figure 13 we compare the measured threshold pressure with two different calculations for L_d = 49 cm (see parameters used in the model in Tables I and II). The first calculations using the measured quality factor Q_2 = 10 underestimate significantly p_{th} but predict the decrease of p_{th} with increasing internal lip pressure up to p_{in} = 9.1 kPa. For higher internal lip pressures, no simulations have been performed because there are no data on the mechanical response of the lips. Above p_{in} = 9.1 kPa the threshold pressure is close to the lung pressure needed to open the lips. Reducing the quality factor Q_2 of the lips by a factor two allows to obtain an excellent fit of p_{th} for p_{in} < 9.1 kPa.

In Figure 14, the corresponding measured and predicted oscillation frequencies are shown for p_{in} = 9.1 kPa as a function of p_l for L_d = 49 cm. Two different values of the

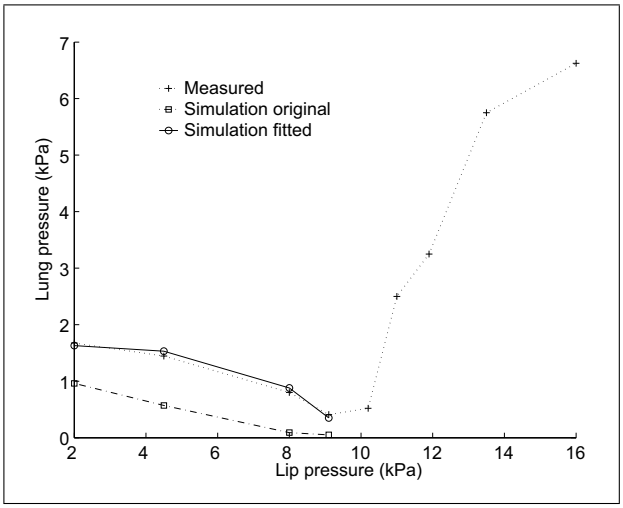

Figure 13. Comparison between measured and predicted threshold pressure p_{th} as a function of the internal lip pressure p_{in} for $L_d = 49$ cm. Both calculations using the measured lip quality factor $Q_2 = 10$ (original) and half this quality factor $Q_2 = 5$ (fitted) are shown.

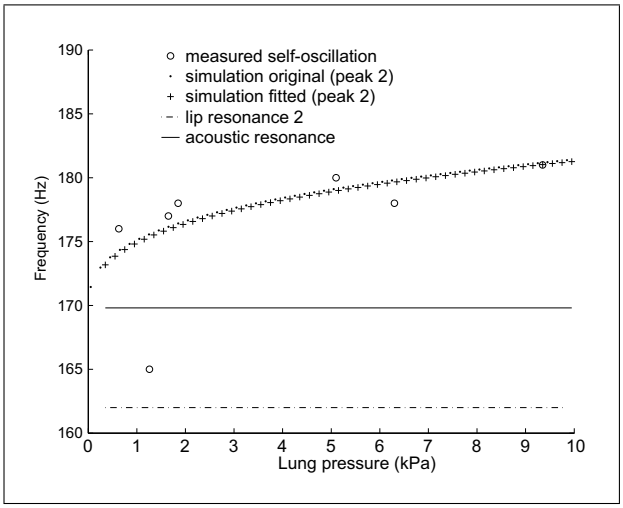

Figure 14. Comparison of measured and predicted oscillation frequency f as a function of the lung pressure p_l for $L_d = 49$ cm and $P_{in} = 9.1$ kPa. Both calculations using the measured lip quality factor $Q_2 = 10$ (original) and half this quality factor $Q_2 = 5$ (fitted) are shown.

Table I. Mechanical data lip-model: average values.

Resonance	f_i (Hz)	Q_i	A_d (m^{2}kg^{-1})
1	80	4	0.03
2	162	10	0.03
3	228	8	-0.03

Table II. Data of the pipes. I: Upstream ($p_{in} = 9.1$ kPa), II: Long downstream, III: Short downstream.

Pipe	Length (cm)	f_i (Hz)	Q_i	Z_i (MPa s m^{-3})
I	36	239	5	3.77
II	49	170	55	39.97
III	16	494	46	33.56

quality factor have been used: the original measured quality factor $Q_2 = 10$ and the quality factor obtained from the fit of the threshold pressure in Figure 13 $Q_2 = 5$. As a reference we also show the quarter-wavelength pipe resonance frequency f_d and the lip resonance frequency f_2.

As expected for an outward-striking behavior the oscillation frequency $f = \Im[\alpha]/2\pi$ is higher than both resonance frequencies. It should be noted that finite amplitude self-sustained oscillation can only be established as a result of non-linear saturation effects. Hence, for $p_l > p_{th}$, the good agreement between theory and experiments indicate that the non-linearities such as the collision of the lips have little influence on the oscillation frequency.

The linear stability analysis allows to predict the threshold values of the lung pressure for which self-sustained oscillations begin and the corresponding frequency of these oscillations. In Figures 15 and 16 these threshold values are plotted together with the measured values for $p_{in} = 9.1$ and 4.5 kPa for the situations with and without downstream pipe respectively.

When the downstream pipe is present, the 1-mass model gives a good prediction of the oscillation frequency (within 10% of the measured values) independent of the choice of mechanical resonance of the lips and of the quality factor. However, the predicted threshold pressure differs significantly from the measured values and is very sensitive to the choice of lip resonance frequency and quality factor. In the situation without downstream pipe self-sustained oscillations are only found when the third resonance is chosen to model the lips. In this case, we obtain a reasonable prediction of the threshold lung pressure but a poor prediction of the oscillation frequency, specially for $p_{in} = 4.5$ kPa. Again the quality factor has a significant influence on the predicted threshold pressure.

The single-mass model fails to predict the observed oscillation frequencies for $L_d = 0$. In such a case $p'_d = 0$ and the upstream resonance frequency $f_u = 240$ Hz has to be invoked. Using f_2 for the lips would then imply that the oscillation frequency f is included between f_2 and f_u. The same is valid for f_3. The theory cannot predict such a behavior, independently of the choice of A_u and A_d. A striking feature observed in Figure 12 is that the transition from an oscillation around the mechanical mode f_3 towards an oscillation around f_2 occurs when the oscillation frequency f approaches the upstream acoustical resonance frequency f_u. Further research should confirm whether this is more than a coincidence.

5.3. Two-mass model

The 2-mass model of Lous *et al.* [6] (see Figure 7) has also been used in an attempt to predict the observed self-sustained oscillations. In that case both the up- and downstream acoustics were taken into account. This yields a model with four degrees of freedom. Linear stability analyses have been carried out using the second and third lip

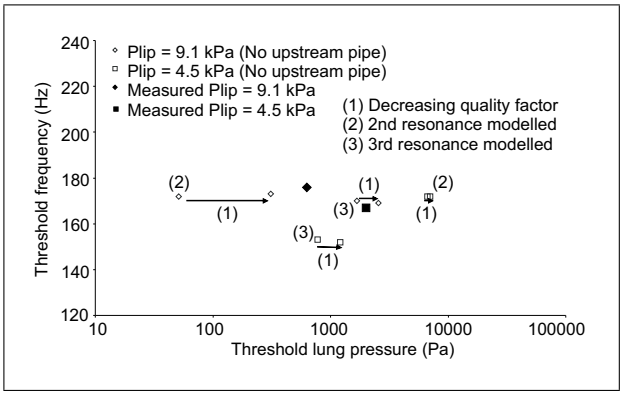

Figure 15. 1-mass model: Comparison of measured and predicted oscillation frequency f vs the threshold lung pressure $(p_l)_{th}$ for $L_d = 49$ cm. The arrow indicates a decreasing quality factor from $Q_2 = 10$ to $Q_2 = 5$.

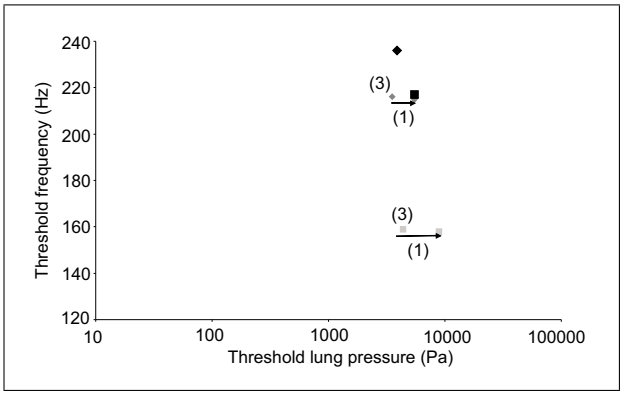

Figure 16. 1-mass model: Comparison of measured and predicted oscillation frequency f vs the threshold lung pressure $(p_l)_{th}$ without downstream pipe ($L_d = 0$). The arrow indicates a decreasing quality factor from $Q_2 = 10$ to $Q_2 = 5$. Legend as in Figure 15.

resonances f_2 and f_3. One would expect the first resonance f_1 to correspond to an essentially three dimensional motion in which water flows from the center of the lips towards the sides. However, this involves a much larger effective mass than a locally two dimensional motion. Hence, it is not surprising that this yields a rather low frequency. A 2-mass model like the one proposed here cannot describe such motions. In actual lips or vocal folds three dimensional motions are also expected to be quite significant [13].

The system parameters needed in equation (7) (k, k_c, m and c) have been determined by curve fitting the measured static response (Figure 3). To his end an iterative trial-and-error procedure has been used. First values for k and k_c were guessed and then the measured lip resonance frequencies (f_2 and f_3) and quality factors from Figure 8 were used to determine m and c. With these parameters the static opening of the lips was predicted using the 2-mass model and visually compared to the measurement. This procedure has been repeated until a good match between predicted and measured static opening was found. The values of the parameters found in this way are summarized in Table I. Two parameters have been varied: the quality factor of the lip resonances, Q_L, and the distance between the two masses, $x_2 - x_1$, in Figure 7 (this distance has been varied keeping the matching of the model to the mechanical properties of Table I). The predicted threshold lung pressure and threshold oscillation frequency are shown in Figures 17 and 18 for the situations with and without downstream pipe respectively. The filled grey symbols correspond to a model with upstream pipe and the empty symbols to a model without upstream pipe.

When the downstream pipe is present, Figure 17, the predicted oscillation frequency is significantly lower than the measured frequency. For a lip pressure $p_{in} = 4.5$ kPa we predict a frequency $f \simeq 165$ Hz while $f \simeq 176$ Hz is observed. For a lip pressure $p_{in} = 9.1$ kPa we predict a frequency $f \simeq 140$ Hz while $f \simeq 165$ Hz is observed. This frequency is rather insensitive to the quality factor but increases when the distance $x_2 - x_1$ between the masses is

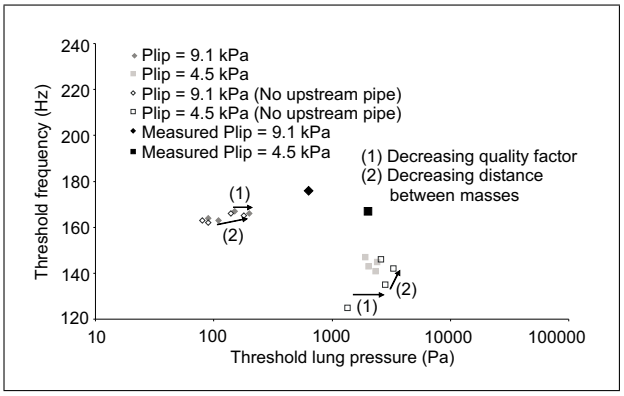

Figure 17. 2-mass model: Comparison of measured and predicted oscillation frequency f vs the threshold lung pressure $(p_l)_{th}$ for $L_d = 49$ cm. The arrow indicates: (1) a decreasing quality factor from $Q_2 = 10$ to $Q_2 = 5$, (2) a decreasing distance $x_2 - x_1$ from 4 to 2 mm for $p_{in} = 9.1$ kPa and from 6 to 4 mm for $p_{in} = 4.5$ kPa.

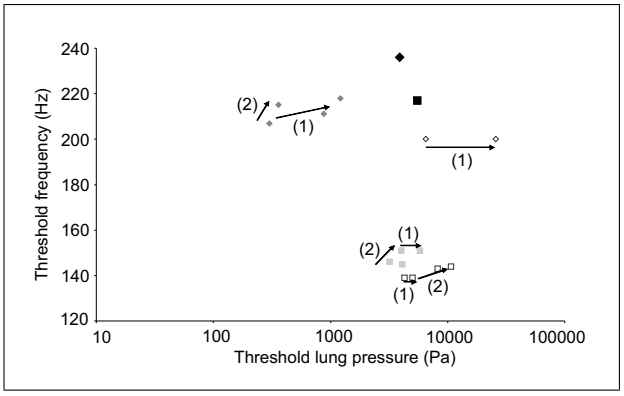

Figure 18. 2-mass model: Comparison of measured and predicted oscillation frequency f vs the threshold lung pressure $(p_l)_{th}$ without downstreampipe ($L_d = 0$). The arrow indicates: (1) a decreasing quality factor from $Q_2 = 10$ to $Q_2 = 5$, (2) a decreasing distance $x_2 - x_1$ from 4 to 2 mm for $p_{in} = 9.1$ kPa and from 6 to 4 mm for $p_{in} = 4.5$ kPa. Legend as in Figure 17.

reduced. The prediction of the threshold lung pressure is reasonable for $p_{in} = 4.5$ kPa but is an order of magnitude

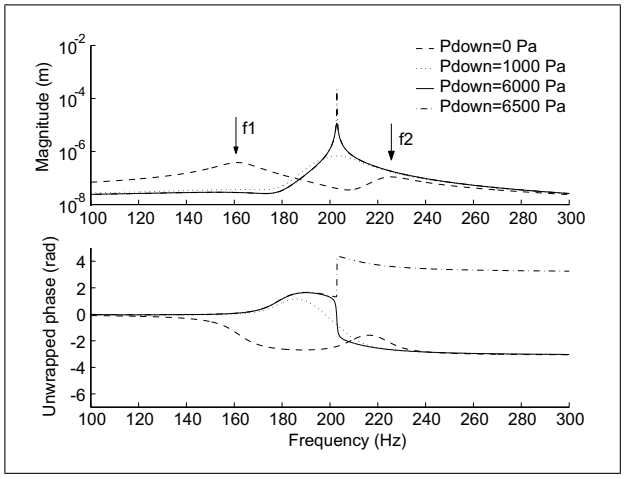

Figure 19. Predicted FRF between downstream pressure and the displacement of mass 2 for several values of the lung pressure p_l without upstreampipe (p_{in} = 9.1 kPa, Q_2 = 10).

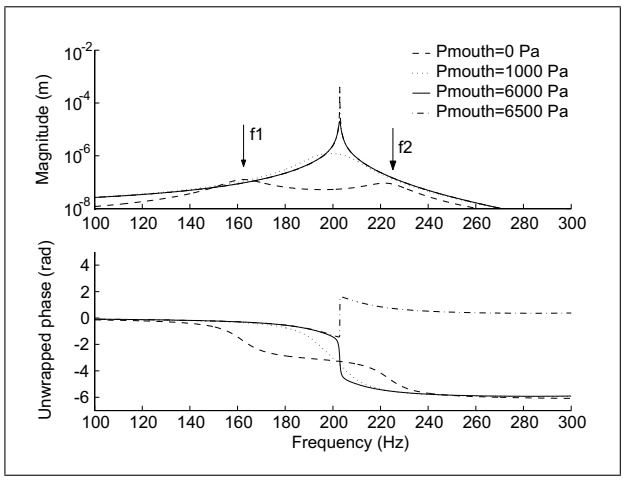

Figure 20. Predicted FRF between upstream pressure and the displacement of mass 2 for several values of the lung pressure p_l without downstreampipe (p_{in} = 9.1 kPa, Q_2 = 10).

too low for p_{in} = 9.1 kPa. For p_{in} = 4.5 kPa the 2-mass model gives a better prediction of the threshold lung pressure than the 1-mass model. However, the prediction of the oscillation frequency is worse. Furthermore, the predicted threshold pressure is sensitive to both the quality factor Q_L and the distance $x_2 - x_1$ between the two masses. Removing the upstream pipe in the model does not change the results significantly.

In the situation without downstream pipe, Figure 18, the 2-mass model gives a poor prediction of the threshold oscillation frequency. The predicted values change when the quality factor Q_L and the distance $x_2 - x_1$ between the masses vary and when the upstream pipe is removed, but the variations are not large. For a lip pressure p_{in} = 4.5 kPa we predict a frequency $f \simeq 140$ Hz while $f \simeq 220$ Hz is observed. For a lip pressure p_{in} = 9.1 kPa the predicted frequency $f \simeq 210$ Hz is significantly lower than the measured frequency $f \simeq 235$ Hz. As for the 1-mass model, the threshold lung pressure is reasonably well predicted for

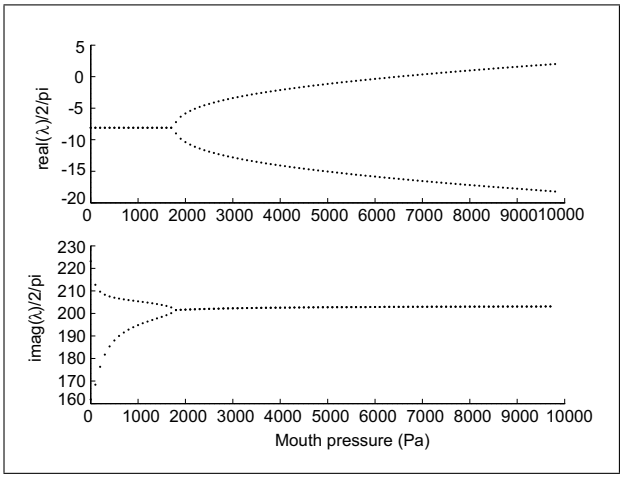

Figure 21. Eigenvalues λ of the 2-mass model without acoustic coupling vs lung pressure p_l without downstreampipe (p_{in} = 9.1 kPa, Q_2 = 10).

p_{in} = 4.5 kPa but not for p_{in} = 9.1 kPa. In the first case the predicted threshold pressure is not very sensitive to variations of Q_L, $x_2 - x_1$ or upstream pipe but for p_{in} = 9.1 kPa the quality factor has a significant influence on the predicted threshold pressure.

It is clear from these figures that the 2-mass model provides little or no improvement in the results compared to the 1-mass model. The 2-mass model has the advantage that two lip resonances can be modeled simultaneously, whereas in the 1-mass model one resonance at a time has to be analyzed. In principle the 2-mass model should be able to predict a transition in oscillation frequency as shown in Figure 12 for L_d = 0, but we have not succeeded to predict such a behavior. Furthermore, the extra complexity of the 2-mass model implies a larger number of parameters that have to be tuned in order to get realistic results. In the light of the presented results, this effort does not seem to be justified.

6. Discussion

In an attempt to through some light on the poor behavior of the 2-mass model, transfer functions have been calculated between the pressure fluctuations downstream and lip opening (displacement of mass 2 in Figure 7) and the pressure fluctuations upstream and lip opening. The results for increasing values of the stationary pressure are shown in Figures 19 and 20 respectively. From those data we will deduce the character of the resonances dis played by our model and compare that with the experimental data.

The frequency response functions (FRF) of the 2-mass model in both Figure 19 and Figure 20 show that the two resonances for $p_l = 0\ Pa$ merge into one resonance at about $p_l = 1000\ Pa$. This can be more clearly seen in Figure 21, where the eigenvalues of the 2-mass model for increasing lung pressure, p_l, are shown. For a lung pressure of approximately 1800 Pa a Hopf bifurcation occurs. As p_l increases damping decreases and between p_l = 6 kPa and

$p_l = 6.5$ kPa the peak becomes unstable. This can be seen by looking at the phase, which shifts from negative to positive. This indicates a shift from positive to negative damping. The change of the resonance from stable to unstable can also be concluded from the eigenvalues in Figure 21. The real part of one of the eigenvalues becomes positive for a lung pressure of about 6500 Pa. If these predicted frequency response functions are compared to the experimental results in Figure 8, it is clear that the predicted threshold pressure for the onset of self-sustained oscillations is almost twice as large as the measured value. However, the Hopf bifurcation can not be found in the measured data from Figure 8.

Looking at the dynamical properties of the model one should be able to see whether the two oscillation modes of the 2-mass model (see Figure 22) behave as inward or outward striking. Since this classification can be confusing the classification proposed by Fletcher and Rossing [4] will be used here. According to Fletcher valves can be classified looking at whether they open or close when the pressure at the upstream or downstream side increases.

In order to establish the inward or outward-striking character of the two resonances modeled in the 2-mass model, the phase of the frequency response functions for $p_l = 0$ Pa has to be analyzed. In Figure 19 we consider the model response for fixed p_u (no upstream pipe). Both resonances have a negative phase and, since the pressure fluctuations are applied downstream, this means that both resonances have an inward-striking character. In other words, the lip opening tends to increase as the downstream pressure increases. Using the classification introduced by Fletcher and Rossing [4] both resonances are (?,+) (the question mark means that we still do not know what the sign is). Looking now at Figure 20 we consider the model for fixed p_d (no downstream pipe). The first resonance has a negative phase and the second resonance has a positive phase (note that the unwrapped phase has been plotted). In this case the pressure fluctuations are applied upstream, which means that the first resonance should have an outward-striking character and the second resonance an inward-striking character. Apparently, for the first resonance, when the pressure either upstream or downstream increases the lip opening increases. According to Fletcher and Rossing [4] this gives a (+,+) character or sideways-striking behavior. The second resonance has a (-,+) or inward-striking behavior.

These results can be compared to the conclusions derived in section 5.1 from the measured frequency response function shown in Figure 8. It was shown there that the second resonance (first in the model) has an outward striking-behavior and the third resonance (second in the model) has an inward-striking behavior. More precisely, the measurements indicate a (?,-) character for the second resonance and a (?,+) character for the third resonance. Therefore the second resonance can only have a (+,-) character, that is an outward-striking behavior. The 2-mass model fails to capture this behavior, since it has been shown that the first resonance in the model (second in the measurements) has a (+,+) character. For the third resonance both (+,+) and (-,+) are possible, but, according to the results of Cullen *et al.* [5] the (-,+) or inward-striking character is more likely, which is correctly predicted by the 2-mass model.

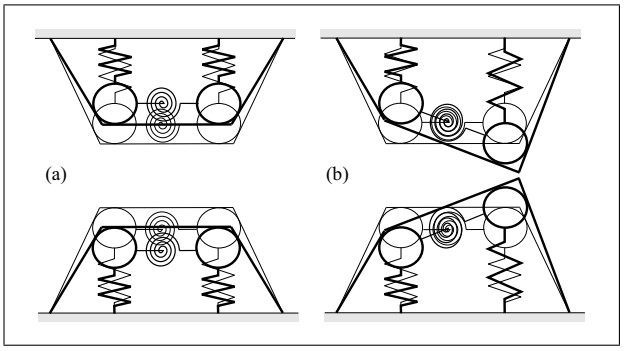

Figure 22. Mode shapes of the 2-mass model. (a) In-phase, (b) Out-of-phase.

This failure of the 2-mass model can be easily explained by looking at the modeshapes that correspond to each of the resonances. For a positive value of the cross-coupling stiffness in Figure 7 the first modeshape corresponds to an in-phase motion of both masses (Figure 22a) and the lip opening will increase when either the upstream or downstream pressure increase. Therefore, this first mode of the 2-mass model has an intrinsic (+,+) character. The second modeshape corresponds to an out-of-phase motion of the two masses (Figure 22b) and, recalling that the lip opening is defined as the displacement of mass 2 in Figure 7, the lip opening will increase when the downstream pressure fluctuations increase and decrease when the upstream pressure fluctuations increase. Therefore, the second mode of the 2-mass model has an intrinsic (-,+) character.

One could argue that the wrong choice of resonances has been made from the experimental data. Suppose the first and second resonance from the measurements had been chosen. According to the measured frequency response functions, both resonances have an outward-striking behavior. The 2-mass model would have modeled them as sideways-striking and inward-striking respectively. Furthermore, it has already been explained in section 5.3 that the first resonance frequency f_1 is very likely to be related to a three dimensional motion of the water in the lips, which cannot be modeled by the 2-mass model proposed here.

From the above results it can be concluded that the 2-mass model has clear intrinsic limitations which could be the reason why no significantly better predictions are obtained when compared to the simpler 1-mass model. One should select alternative low dimensional models which do not display such problems [14, 15, 16, 17].

7. Conclusions

Globally our results agree with those of Cullen *et al.* [5] indicating that the upstream acoustics is not crucial for

the behavior of lips buzzing near the oscillation threshold. The single mass model performs well when considering conditions in which there is a strong coupling between the lips and the downstream acoustics, as occurs in musical instruments. This model combined with a linear stability analysis does not only predict the threshold behavior but also the dependence of the oscillation frequency on the lung pressure. This indicates that non-linearities introduced by features such as the collision of the lips are not crucial for these features. Some differences observed between our results and the work of Cullen are probably due to the difference in mechanical boundary conditions. This confirms the importance of those boundary conditions. In our experiments the lips were "free" while in brass instruments the lips are pressed against a mouth-piece which determines the mechanical boundary conditions of the oscillator. Our artificial lips have a poor oscillation behavior without downstream pipe.

Attempts to apply the simplified 2-mass model of Lous *et al.* [6] to our lips, have not improved the results with respect to the 1-mass model. Furthermore, minor modifications in the geometry assumed for the 2-mass model were found to have a strong impact on the predicted lung pressure at the oscillation threshold, which makes this model unpractical to use.

Further analysis of the 2-mass model has shown that there are intrinsic limitations of this model which prevent the correct modeling of the observed phenomena. The two modes of the model have respectively a sideways-striking behavior (+,+) and inward-striking behavior (-,+) following Fletcher's classification. Experimentally the artificial lips display outward-striking (+,-) and inward-striking (-,+) dominating modes. A low dimensional lip model should be selected according to this property. It seems quite useless to improve the modeling of the fluid dynamics without using a more realistic mechanical description of the lips. Once the linear behavior of the lip model fits better the actual lip behavior, one should pay attention to the collision model which determines the non-linear response of the system.

8. Acknowledgements

The authors would like to thank Freek van Uittert, Jan Willems, Remi Zorge, Niels Driessen and Ries Schellekens for their valuable contribution to the experiments.

Appendix – Derivatives of the forces

In the following equations $\overline{\Delta P} = \overline{P_d} - \overline{P_u}$, b is the lip length, $y_0 = d_d/2$ is the pipe radius and x_0, x_1, x_2 and x_3 are parameters of the 2-mass model shown in Figure 7. The numerical values used in the simulations are: $x_0 = 0$ mm and $x_3 = 12$ mm. The values of b and d_d are given in section 2 and $\overline{\Delta P}$, x_1 and x_2 have been varied as explained in section 5.

The derivatives with respect to y_1 and y_2 are:

$$\frac{\partial F_1}{\partial y_1} = \left(\frac{\partial F_1}{\partial y_1}\right)_1 + \left(\frac{\partial F_1}{\partial y_1}\right)_2,$$

with

$$\left(\frac{\partial F_1}{\partial y_1}\right)_1 = 2b\overline{\Delta P}(x_1 - x_0)\frac{y_2^2}{(y_1 - y_0)^3} \left(\ln\frac{y_1}{y_0} + \frac{y_0 - y_1}{y_1} - \frac{1}{2}\left(\frac{y_0 - y_1}{y_1}\right)^2\right),$$

$$\left(\frac{\partial F_1}{\partial y_1}\right)_2 = \begin{cases} 2b\overline{\Delta P}(x_2 - x_1)\frac{y_2^2}{(y_2 - y_1)^3} \left(\ln\frac{y_2}{y_1} - \frac{y_2 - y_1}{y_1} + \frac{1}{2}\left(\frac{y_2 - y_1}{y_1}\right)^2\right) & \text{for } y_1 \neq y_2, \\ b\overline{\Delta P}(x_2 - x_1)\frac{y_2^2}{y_1^3} & \text{for } y_1 = y_2, \end{cases}$$

$$\frac{\partial F_1}{\partial y_2} = \left(\frac{\partial F_1}{\partial y_2}\right)_1 + \left(\frac{\partial F_1}{\partial y_2}\right)_2,$$

with

$$\left(\frac{\partial F_1}{\partial y_2}\right)_1 = -2b\overline{\Delta P}(x_1 - x_0)\frac{y_2}{(y_1 - y_0)^2}\left(\ln\frac{y_1}{y_0} + \frac{y_0}{y_1} - 1\right),$$

$$\left(\frac{\partial F_1}{\partial y_2}\right)_2 = -\frac{y_1}{y_2}\left(\frac{\partial F_1}{\partial y_1}\right)_2,$$

$$\frac{\partial F_2}{\partial y_1} = \begin{cases} -2b\overline{\Delta P}(x_2 - x_1)\frac{y_2^2}{(y_2 - y_1)^3} \left(\ln\frac{y_2}{y_1} - \frac{y_2 - y_1}{y_1} - \frac{1}{2}\frac{(y_2 - y_1)^2}{y_1 y_2}\right) & \text{for } y_1 \neq y_2, \\ \left(\frac{\partial F_1}{\partial y_1}\right)_2 & \text{for } y_1 = y_2, \end{cases}$$

$$\frac{\partial F_2}{\partial y_2} = \begin{cases} -\frac{y_1}{y_2}\frac{\partial F_2}{\partial y_1} & \text{for } y_1 \neq y_2, \\ \left(\frac{\partial F_1}{\partial y_2}\right)_2 & \text{for } y_1 = y_2. \end{cases}$$

The derivatives with respect to p_d and p_u are:

$$\frac{\partial F_1}{\partial p_u} = \left(\frac{\partial F_1}{\partial p_u}\right)_1 + \left(\frac{\partial F_1}{\partial p_u}\right)_2,$$

with

$$\left(\frac{\partial F_1}{\partial p_u}\right)_1 = \frac{1}{2}b(x_1 - x_0)\left[1 - 2\frac{y_2^2}{(y_1 - y_0)^2}\left(\ln\frac{y_1}{y_0} + \frac{y_0}{y_1} - 1\right)\right],$$

$$\left(\frac{\partial F_1}{\partial p_u}\right)_2 = \begin{cases} \frac{1}{2}b(x_2 - x_1)\left[1 + 2\frac{y_2^2}{(y_2 - y_1)^2}\left(\ln\frac{y_2}{y_1} - \frac{y_2}{y_1} + 1\right)\right] & \text{for } y_1 \neq y_2, \\ 0 & \text{for } y_1 = y_2, \end{cases}$$

$$\frac{\partial F_1}{\partial p_d} = \left(\frac{\partial F_1}{\partial p_d}\right)_1 + \left(\frac{\partial F_1}{\partial p_d}\right)_2,$$

with

$$\left(\frac{\partial F_1}{\partial p_d}\right)_1 = b(x_1 - x_0)\frac{y_2^2}{(y_1 - y_0)^2}\left(\ln\frac{y_1}{y_0} + \frac{y_0}{y_1} - 1\right),$$

$$\left(\frac{\partial F_1}{\partial p_d}\right)_2 = \begin{cases} -b(x_2 - x_1)\frac{y_2^2}{(y_2 - y_1)^2}\left(\ln\frac{y_2}{y_1} - \frac{y_2}{y_1} + 1\right) & \text{for } y_1 \neq y_2, \\ \frac{1}{2}b(x_2 - x_1) & \text{for } y_1 = y_2, \end{cases}$$

$$\frac{\partial F_2}{\partial p_u} = \begin{cases} \frac{1}{2}b(x_2-x_1)\left[1-2\frac{y_2^2}{(y_2-y_1)^2}\left(\ln\frac{y_2}{y_1}+\frac{y_1}{y_2}-1\right)\right] & \\ \qquad\qquad \text{for } y_1 \neq y_2, & \\ 0 \qquad\qquad \text{for } y_1 = y_2, & \end{cases}$$

$$\frac{\partial F_2}{\partial p_d} = \begin{cases} b(x_2-x_1)\frac{y_2^2}{(y_2-y_1)^2}\left(\ln\frac{y_2}{y_1}+\frac{y_1}{y_2}-1\right) & \\ \quad +\frac{1}{2}b(x_3-x_2) \qquad \text{for } y_1 \neq y_2, & \\ \frac{1}{2}b(x_3-x_1) \qquad \text{for } y_1 = y_2. & \end{cases}$$

References

[1] . Helmholtz: On the sensation of sound. Translated by A. J. Ellis. reprinted by Dover, New York, 1954.

[2] S. J. Elliott, J. M. Bowsher: Regeneration in brass wind instruments. J. Sound Vib. **83** (1982) 181–217.

[3] S. Yoshikawa: Acoustical behavior of brass player's lips. J. Acoust. Soc. Am. **97** (1995) 1929–1939.

[4] N. H. Fletcher, T. D. Rossing: The physics of musical instruments. Second edition. Springer-Verlag, New York, 1998.

[5] J. S. Cullen, J. Gilbert, D. M. Campbell: Brass instruments: linear stability analysis and experiments with an artificial mouth. Acta Acustica united with Acustica **86** (2000) 704–724.

[6] N. J. C. Lous, G. C. J. Hofmans, R. N. J. Veldhuis, A. Hirschberg: A symmetrical two-mass vocal-fold model coupled to vocal tract and trachea, with application to prosthesis design. Acta Acustica united with Acustica **84** (1998) 1135–1150.

[7] J. Gilbert, S. Ponthus, J. F. Petiot: Artificial buzzing lips and brass instruments: experimental results. J. Acoust. Soc. Am. **104** (1998) 1627–1632.

[8] C. Vergez: Trompette et trompetiste: un système dynamique non-linéaire, analyse, modélisation, simulation dans un contexte musical. PhD thesis, Institut de Recherche et de Coordination Acoustique Musicale (IRCAM), Paris, 2000.

[9] C. E. Vilain, X. Pelorson, A. Hirschberg, L. Le Marrec, W. Op't Root, J. Willems: Contribution to the physical modeling of the lips: Influence of the mechanical boundary conditions. Acta-acustica united with Acustica **89** (2003) 882–887.

[10] A. D. Pierce: Acoustics: an introduction to its physical principles and applications. 1989 ed., 2nd print. McGraw-Hill, London, 1991.

[11] M. C. A. M. Peters, A. Hirschberg, A. J. Reijnen, A. P. J. Wijnands: Damping and reflection coefficient measurements for an open pipe at low Mach numbers and low Helmholtz numbers. Journal of Fluid Mechanics **256** (1993) 499–534.

[12] S. Yoshikawa, G. R. Plitnik: An experimental investigation of the phase difference between lip vibration and acoustic pressure in brass instrument mouthpieces. J. Acoust. Soc. Am. **94** (1993) 1834.

[13] J. G. Svec, J. Horácek, F. Sram, J. Vesely: Resonance properties of the vocal folds: In vivo laryngoscopic investigation of the externally excited laryngeal vibrations. J. Acoust. Soc. Am. **108** (2000) 1397–1407.

[14] K. Ishizaka, J. L. Flanagan: Synthesis of voiced sounds from a two-mass model of the vocal folds. Bell Syst. Tech. J. **51** (1972) 1233–1268.

[15] I. R. Titze, B. H. Story: Rules for controlling low-dimensional vocal fold models with muscle cavitation. J. Acoust. Soc. Am. **112** (2002) 1064–1076.

[16] S. Adachi, J. Yu: Two-dimensional model of vocal fold vibration for sound synthesis of voice and soprano singing. J. Acoust. Soc. Am. **117** (2005) 3213–3224.

[17] C. Drioli: A flow waveform-matched low-dimensional glottal model based on physical knowledge. J. Acoust. Soc. Am. **117** (2005) 3184–3195.